

EFFECT OF THE VARIATION OF CUTTING PARAMETERS IN SURFACE INTEGRITY IN TURNING PROCESSING OF AN AISI 304 AUSTENITIC STAINLESS STEEL¹

Daniel Alexander Flórez Orrego²
Luis Bernardo Varela Jiménez²
Julian David Escobar Atehortua²
Diana Maria López Ochoa²

Abstract

This paper focuses in understanding the effect of the variation of cutting speed and feed rate in surface integrity and microstructural changes in turning of AISI 304 using cemented carbide tool. Feed rates between 0.15 mm rev⁻¹ and 0.6 mm rev⁻¹ and cutting speeds between 40 m min⁻¹ and 120 m min⁻¹ were used. Depth of cut, lubrication conditions and cutting tool material were set as constants. Different roughness parameters were analyzed in order to describe the effect of cutting parameters on surface integrity. Tool wear and chip structure were studied too. Results showed that hybrid roughness parameters such as R_{pk} , R_{vk} and R_p/R_v described the topography of the turned surfaces in a better way, giving relevance to the peak formation. It was found that for austenitic stainless steel and under these tested conditions, the evaluation of surface integrity only through roughness measurements may be unsatisfactory, since high amounts of micro-defects such as voids and pits were found for the lowest roughness values.

Keywords: Turning; Austenitic stainless steel; Surface integrity; Roughness parameters.

¹ Technical contribution to the First International Brazilian Conference on Tribology – TribobR-2010, November, 24th-26th, 2010, Rio de Janeiro, RJ, Brazil.

² Tribology and surfaces laboratory GTS- National University of Colombia, Medellín
daflorezo@unal.edu.co, lbvarela@unal.edu.co, jdscobaa@unal.edu.co, dmlopez3@unal.edu.co

1 INTRODUCTION

Austenitic stainless steels are characterized by their high corrosion and oxidation resistance, what led to its wide use in different aggressive environments. In spite of these properties, problems such as poor surface finishing and high tool wear are common in machining of this steel.⁽¹⁾ Their low thermal conductivity, low yield strength and metastable microstructure cause that austenitic stainless steels become gumminess during machining, showing a tendency to produce long and stringy chips, to cause seizure, to form a built-up edge on the cutting tool, and to impair surface integrity and tool life.^(2,3) In addition, the transformation to martensite due to plastic deformation and its low stacking fault energy leads to work hardening, what is recognized to be other characteristic that impairs their machinability.^(4,5)

Ihsan et al. carried out turning tests on AISI 304 austenitic stainless steel to determine the optimum machining parameters. They found a decrease in tool wear and an increase in the surface roughness with decreasing the cutting speed, owing to the occurrence of built-up-edge at lower cutting speeds.⁽⁶⁾ Similarly, Cebeli investigated the machining characteristics of an AISI 304 austenitic stainless steel in turning processes. They found that the surface roughness increased when the depth of cut and feed rate were increased; while the cutting speed had an inverse influence.⁽⁷⁾

Lin performed a research to evaluate the behavior of the austenitic stainless steel in high speed turning. He found that the surface roughness values decreased along with the feed rate. However, when the feed rate was smaller than a critical value, the chatter occurred and the surface roughness of the work piece increased. Furthermore, he found that the higher the cutting speed the higher the cutting temperature of cutting tool, causing softening of the cutting tool and deterioration of the work piece surface roughness.⁽⁸⁾

Many works have been developed in this topic, most part of them assess the effect of parameters on roughness and tool wear, but is not evaluated from the tribological point of view. Since cutting operations could be seen as a controlled wear process, the study of this problem from tribology could provide new elements to understand the phenomena involved during cutting and improve the quality of machined austenitic stainless steel pieces.^(2,9,10)

In this work, some surface integrity characteristics are studied as a function of machining conditions, bearing in mind the piece, the tool and the environment as part of a tribosystem. Some statistical parameters as R_a , R_q , R_{sk} , R_{ku} , R_p/R_v , R_{pk} and R_{vk} were studied, and observation of surface and sub-surface modifications was taken into account to analyze the results.

2 EXPERIMENTAL PROCEDURE

2.1 Materials

AISI 304 austenitic stainless steel bars with 240 mm in length and 25.4 mm in diameter were first annealed to 1100°C during 3h, and then slowly cooled down to remove residual stresses from prior manufacturing processes. The nominal chemical composition of the bars is presented in Table 1. The microstructure was composed by austenitic grains and annealed twins and the average hardness value was 180±5 HV.

Table 1. Nominal chemical composition of AISI 304 Stainless steel (wt-%)

	C	Cr	Ni	Si	Mn	P	S
AISI 304	0.07	18.49	8.15	0.57	0.76	0.03	0.009

2.2 Machining tests

Turning operations were carried out in a CNC lathe, using commercial grade CNMG 120408 MM 2025 WC/Co TiN coated carbide cutting tools and a Cimcool Cimtech 500 soluble coolant. Machined samples were 20 mm long and 23.4 mm in diameter as shown in Figure 1. Throughout experiments, the depth of cut was kept constant at 1.0 mm, and feed rates were set at 0.15 mm rev⁻¹, 0.3 mm rev⁻¹ and 0.6 mm rev⁻¹. The cutting speeds used during the machining tests were 40 m min⁻¹, 80 m min⁻¹ and 120 m min⁻¹. The selection of machining conditions was made according to cutting tool manufacturer’s recommendations, literature reviews and parameters used in stainless steel cutting industry. In order to avoid any tool wear effect on the surface integrity results, a new flank was used to perform each test. The cutting conditions used are summarized in Table 2.

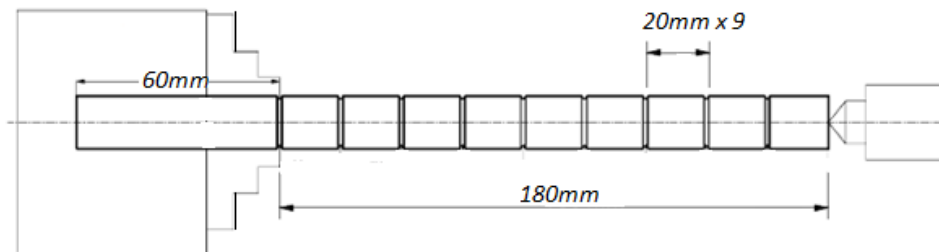


Figure 1. Workpiece and sample’s dimensions.

Table 2. Cutting conditions for the experimental procedure

Cutting Tool	CNMG 120804 MM 2025
Cutting speed V (m min ⁻¹)	40, 80, 120
Depth of cut (mm)	1
Feed rate (mm rev ⁻¹)	0.15, 0.3, 0.6
Tool geometry	Approach angle: 95°; side rake angle: -6°; Back rake angle: -6°; End relief angle: 6°; Side relief angle: 6°

2.3 Laboratory Tests

Changes in surface topography of the samples after machining tests were monitored with the aid of a stylus profilometer, with tip radius of 1µm and resolving power of 0.01µm. A cutoff length of $\lambda=0.8\text{mm}$ was selected for all the measurements according to ISO 4288 standard, thus the total traveling length used was 7.2mm (0.4mm pre-travel+6.4mm evaluation length+0.4mm post-travel).

Roughness parameters R_a , R_q , R_p , R_v , R_{sm} , R_{sk} , R_{pk} , R_{vk} and Abbot-Firestone curves following ISO 4287 standard were used to characterize the surfaces. Analytical definitions of roughness parameters are shown in figure 2. R_a is the mean height of the roughness profile, R_q is the root mean square of the roughness profile heights, R_{sk} is the third central moment of the probability density function measured over the assessment length and used to measure the symmetry of the profile about the mean line, R_{ku} is the fourth central moment of the probability density function measured

over the assessment length and describes the sharpness or flatness of the probability density of the profile, R_{sm} is the mean spacing between profile peaks at the mean line, R_p and R_v are defined as the maximum depth and maximum height of the profile above and below mean line, respectively. The reduced peak height R_{pk} is the average height of the protruding peaks above the roughness core profile and in the same way, the reduced valley depth R_{vk} is the average depth of the profile valleys projecting through the roughness core profile. Abbott Firestone curve or bearing area curve is defined as the percentage of solid material of the profile lying at a certain height; it is useful as an indicator of effective contact area in the surface.

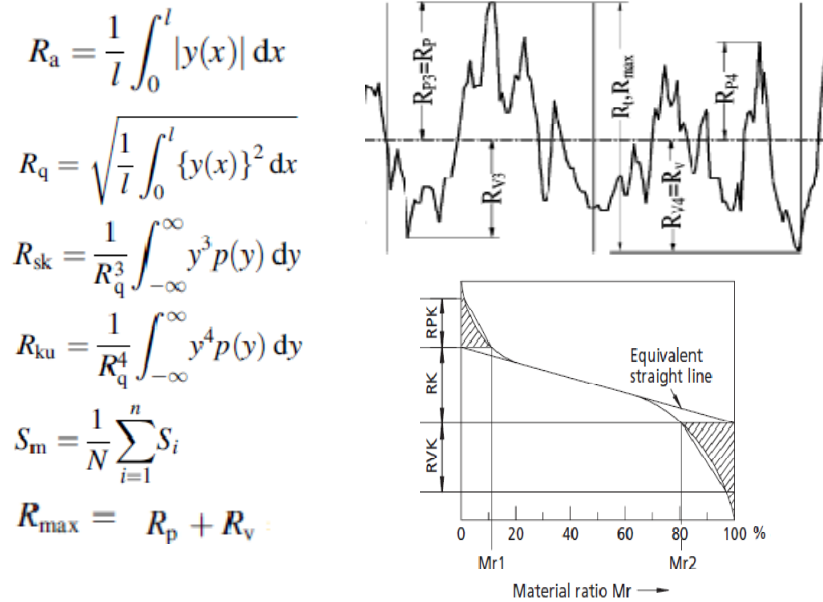


Figure 2. Analytical and graphical definitions of roughness parameters.⁽¹¹⁾

The machined samples selected for metallographic analysis were mounted, mechanically polished and etched with a 10% oxalic acid – water solution during 60 seconds at 6V DC to reveal the microstructure after the tests. The samples were observed with a Nikon Eclipse LV100 Light Optical Microscope (LOM) and a JEOL JSM 5910LV Scanning Electron Microscope (SEM). Three-dimensional reconstructions of machined surfaces were performed by processing digital LOM images taken with height increments of 1µm. Chip structures and cutting tool edges were analyzed using a Nikon SMZ1500 stereomicroscope in order to identify the wear mechanisms and their severity. A Shimadzu microhardness tester with an applied load of 25 g and hold time of 10 s was used to measure the Vickers microhardness of the deformation layer. The spacing between two measuring points was at least 20 µm and the accuracy of the measurement was within ±10 HV.

3 RESULTS AND DISCUSSION

3.1 Surface Roughness Characterization

Measurements of R_a , R_q , R_{sk} and R_{ku} parameters as function of cutting speed and feed rate are shown in Figure 3a and b. It can be seen that feed rate was the most influencing parameter affecting these roughness values, and that the behavior of R_a

and R_q is similar. As it was expected, surface roughness had a negligible variation with the cutting speed. Feed rates of 0.6 mm rev^{-1} showed both the highest R_a and R_q values, while the samples machined with the lowest feed rate of 0.15 mm rev^{-1} showed the lowest roughness values, as shown in Figure 3a. Hence, it is possible to conclude that, for these test conditions, surface finishing is improved when feed rate is reduced.

On the other hand, there were not found any significant variation of the R_{sk} and R_{ku} values with the combination of cutting speeds and feed rates used in this experimental procedure. This is shown in Figure 3b for all the machined samples. Positive values of R_{sk} are related to prominent peaks and shallow valleys along the measured length.

Likewise, the probability density functions for the evaluated conditions exhibit a similar shape, as indicated by R_{ku} . This result indicates that height distribution was not affected by process parameters and it is a process characteristic. Nevertheless, the fastest cutting speed and the lowest feed rate (120 m min^{-1} and 0.15 mm rev^{-1}) showed the flattest surface.

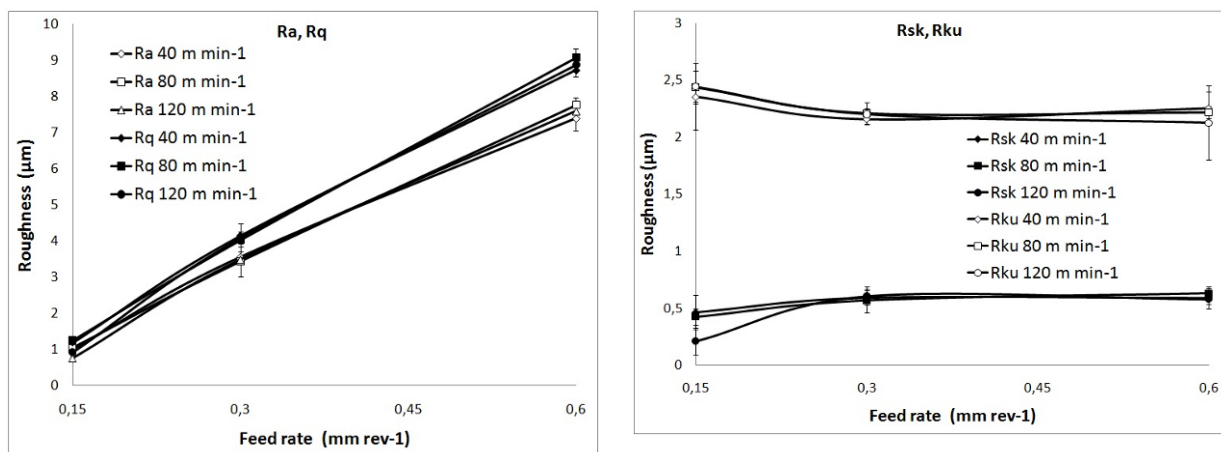


Figure 3. Roughness parameters as function of machining conditions a) R_a and R_q b) R_{ku} and R_{sk} as a function of feed rate and cutting speed.

Other topographic factors describing surface finishing are related to the peak-to-valley ratio R_p/R_v (Figure 4a), hybrid parameters of the bearing area curve R_{pk} and R_{vk} (Figure 4b) and Abbott-Firestone curves (Figure 5a, b, c). Figure 4a shows that the lower the feed rate the lower the ratio R_p/R_v because of the reduction of peak heights related to the depth of valleys. Reduced peak height (R_{pk}) in Figure 4b also shows a preference in the formation of peaks when using higher feed rates, while the reduced valley depths (R_{vk}) remained constant. Hence, the smoother surface finishing corresponds to a feed rate of 0.15 mm rev^{-1} since distance from reduced peak heights to reduced valley depths was the shortest for all cutting speeds.

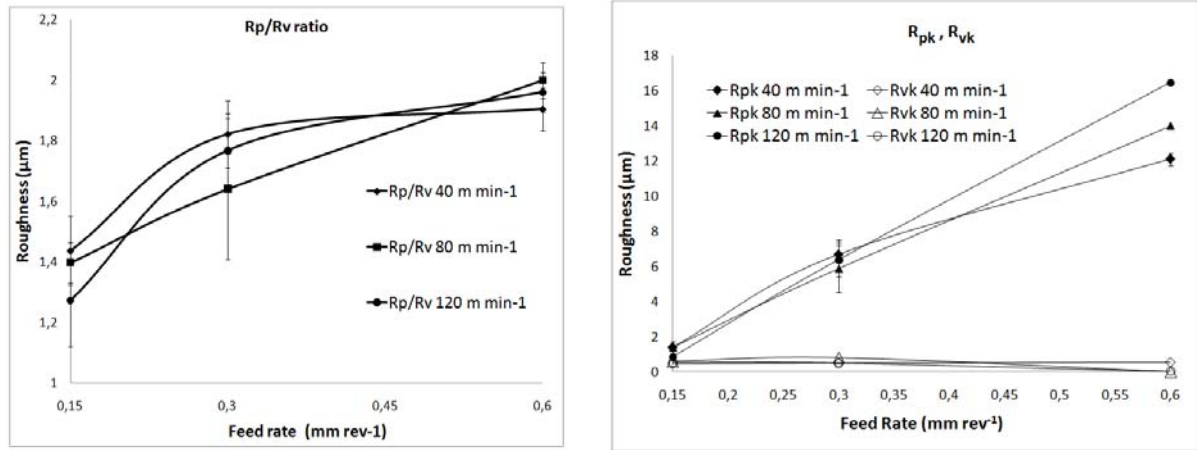


Figure 4. Hybrid roughness parameters as function of machining conditions a) R_p/R_v ratio and b) R_{pk} and R_{vk} as function of feed rate and cutting speed.

Figure 5 shows the Abbott-Firestone curves of surfaces obtained with a constant cutting speed of 120 m min^{-1} and variation in feed rate. These curves show that the total height of Abbott-Firestone curve increased from $4.992 \mu\text{m}$ to $31.597 \mu\text{m}$ when feed rate is increased. These factors indicated that, during turning operations, removal of peaks is the most important factor determining the quality of a flat surface. Figure 6 shows 3D images reconstructed from surfaces processed with three different feed rates and a constant cutting speed of 120 m min^{-1} . The shape of the Abbott-Firestone curves and the 3D reconstruction evidenced the degree of flatness and wavelength along the measured length. It is possible to differentiate a continuous rising in amplitudes and wavelengths in machined surfaces as the feed rate is increased, as well as described by the roughness values presented before. Feed rate of 0.6 mm rev^{-1} showed the highest waviness (Figure 6a) and presented a peak-to-valley ratio of 2, evidencing that roughness profile, and therefore surface quality, are principally affected by a preferential formation of peaks. In addition, a feed rate of 0.15 mm rev^{-1} , which visually seems to have the best surface finish, showed the lowest peak-to-valley ratio of 1.2, indicating that this cutting condition generates the flattest and most homogeneous surface, as shown in Figure 6c.

As it was expected, R_{sm} showed a consistent relationship with the feed rate while cutting speed did not evidence a noticeable influence on these values as shown in Table 3. The R_a , R_q , R_p , R_v , R_{vk} and R_{pk} values were directly affected by reducing the mean roughness spacing R_{sm} using lower feed rates. This fact is therefore related with an improvement on surface finishing of machined samples.

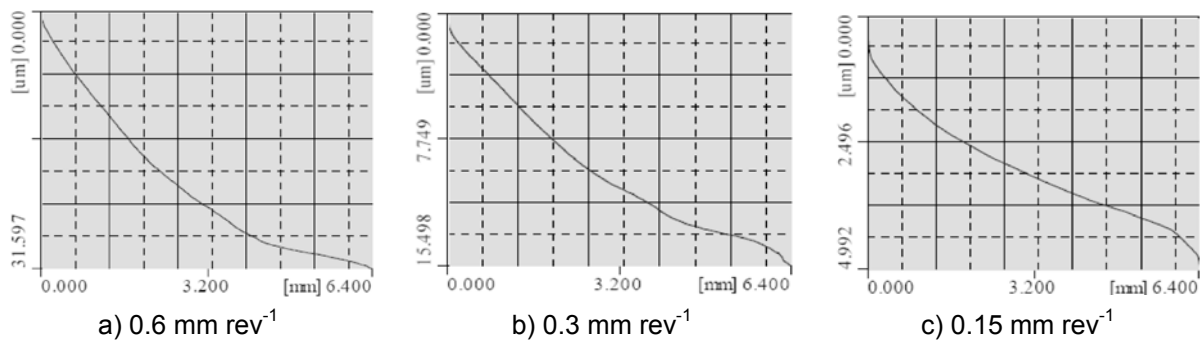


Figure 5. Abbott-Firestone curves for a constant cutting speed of 120 m min^{-1}



a) 0.6 mm rev⁻¹ b) 0.3 mm rev⁻¹ c) 0.15 mm rev⁻¹
Figure 6. Digital surface reconstruction for a constant cutting speed of 120m min⁻¹

Table 3. R_{sm} values for different cuttings conditions.

Cutting Speed (m min ⁻¹)	Feed rate (mm rev ⁻¹)		
	0.15	0.3	0.6
40 (m min ⁻¹)	0.147±0.010	0.299±0.003	0.594±0.02
80 (m min ⁻¹)	0.146±0.025	0.304±0.015	0.6±0.024
120 (m min ⁻¹)	0.179±0.02	0.303±0.013	0.601±0.017

Finally for this range of cutting conditions, it was found that the best surface finishing characterized through roughness measurements was described simultaneously by the lowest values of R_a, R_q, R_{pk}, R_{vk}, R_{sm} and R_p/R_v. It was found that hybrid roughness parameter R_p/R_v, describes in a better way the topography of the turned surfaces giving relevance to the peak formation.

3.2 Comparison of Experimental Results with Theoretical Model

Conventionally, the quality of a machined surface is assessed through R_a measurements, and it is common to find expressions that attempt to predict it using the tool radius and the feed rate. However, when comparing the experimental results and the theoretical model for a rounded tool tip^(9,12,13) for the maximum roughness values R_t and the mean roughness R_a, it was found that only at low feed rates, the maximum roughness values R_t fit to those values predicted by the conventional model. There was not any coincidence between the average roughness, R_a, predicted by the mathematical method and the experimental results obtained in this work. This result is shown in Figure 7.

It is possible that theoretical models that relate feed rate with R_a and R_t fit adequately to experimental results just for higher cutting speeds. Davim suggested that a critical cutting speed is around 200 m min⁻¹.⁽¹⁴⁾

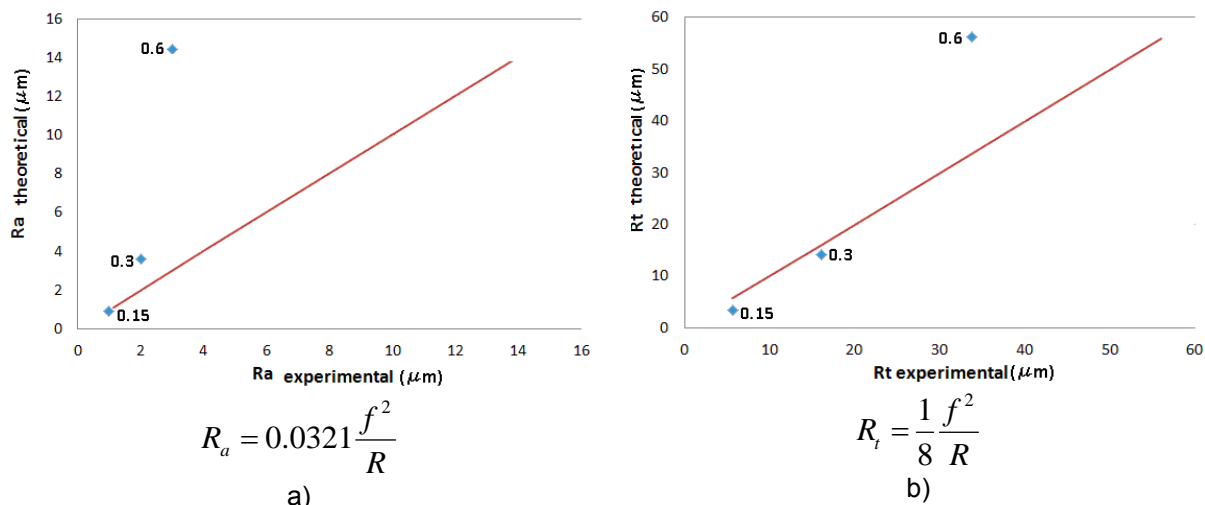


Figure 7. a) Comparison between values of R_a obtained theoretically (red line) and experimentally (dots) and b) Comparison between values of R_t obtained theoretically and experimentally. f = feed rate, R=Tool radius.

3.3 Surface and Subsurface Damage

The observation of cross sections of machined samples revealed that the cutting process affect the sub-surfaces considerably; extensive plastic deformation of grains near the surface and the formation of a thin hardened layer and slip bands were observed (Figure 8a). This microstructural change affected the surface hardness. Figure 8b shows the variation of microhardness as a function of depth for the three feed rates evaluated in this work at 120 m min^{-1} . Some authors have identified a “white layer” in the surface of austenitic stainless steels under severe plastic deformation.⁽¹⁵⁻¹⁸⁾ However, this layer was not observed in this case.

According to Figure 8b, a work hardened layer with thickness between 60 and 70 μm beneath the machined surface caused an increase in hardness value in comparison with the average value of the base material.

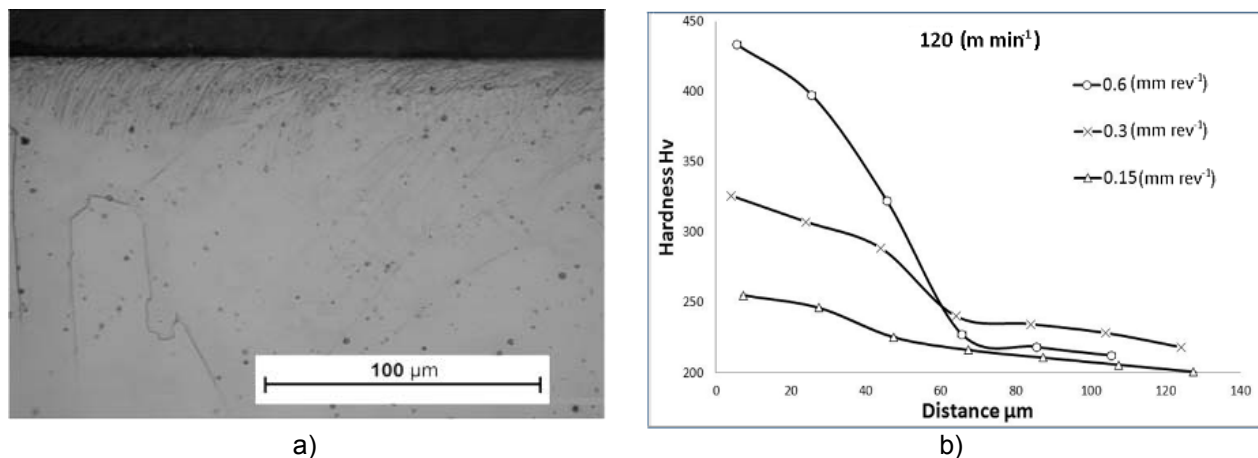


Figure 8. a) LOM microstructure for a cutting speed of 120 m min^{-1} and a feed rate of 0.3 mm rev^{-1} b) Variation of micro-hardness beneath the machined surface when machining at 120 m min^{-1} .

Figure 8b shows that higher values of hardness were measured in the sample processed with the highest feed rate (0.6 mm rev^{-1}) for the same cutting speed of 120 m min^{-1} . The overall highest hardness recorded was $434 \text{ Hv}_{25\text{g}}$. This figure also suggests that the minimal increment in hardness value was exhibited when the feed rate was 0.15 mm rev^{-1} at a cutting speed of 120 m min^{-1} . The lowest hardness measured in the region near to surface was $236 \text{ Hv}_{25\text{g}}$ when machining at a cutting speed of 40 m min^{-1} and feed rate of 0.15 mm rev^{-1} .

Figure 9 shows SEM micrographs of the surface after machining tests. Feed marks are emphasized by black arrows and surface damage by white arrows. Feed marks occur as result of formation of lips on the machined surface by lateral plastic flow of material during the cutting process. These lips result in higher surface roughness values and higher residual stress levels.⁽¹⁹⁾ Images of machined surfaces showed in a) and d) evidenced larger deformation along the feed marks (extreme conditions), while b) and d) showed detached material marks. In spite of that, roughness values presented earlier did not show any match with these observations.

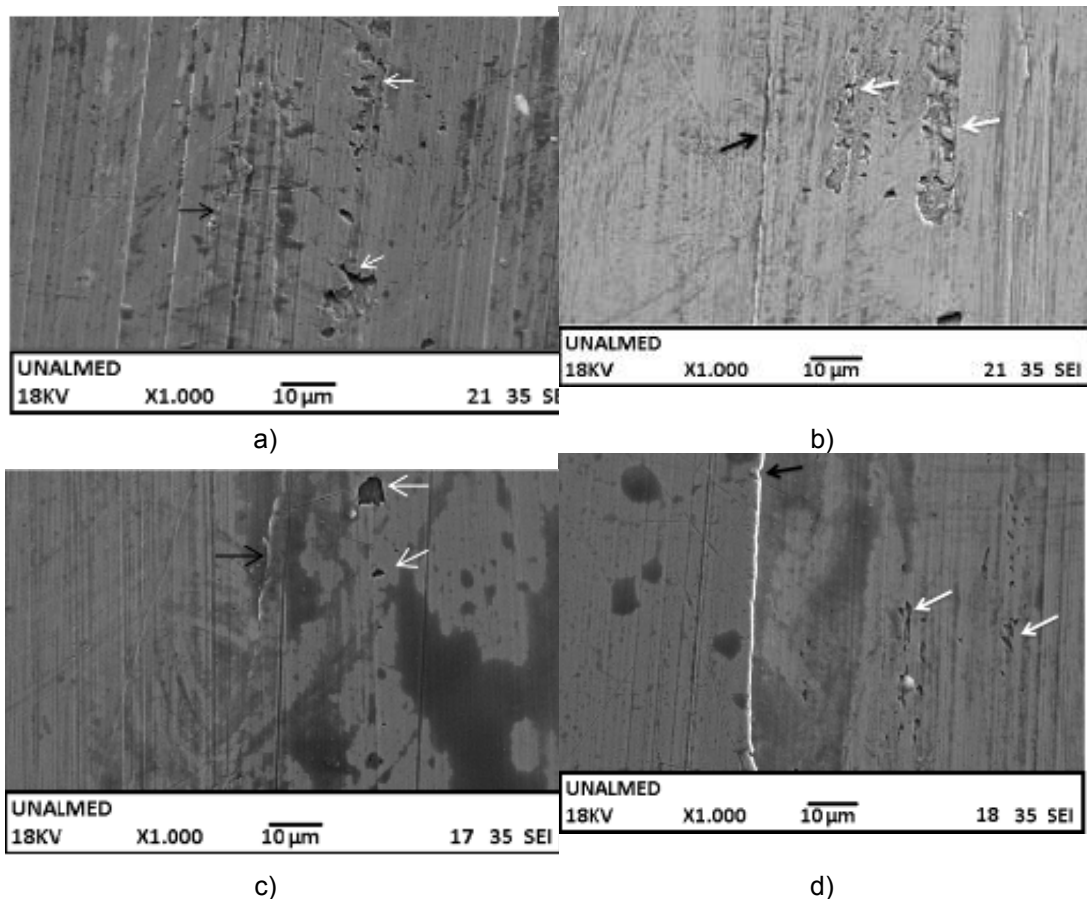


Figure 9. SEM micrographs. Surface generated at different cutting conditions a) 0.15 mm rev^{-1} and 40 m min^{-1} b) 0.15 mm rev^{-1} and 120 m min^{-1} c) 0.6 mm rev^{-1} 40 m min^{-1} and d) 0.6 mm rev^{-1} and 120 m min^{-1} .

For constant feed rate, increasing the cutting speed will generate more heat what could produce more plastic deformation and micro-pitting⁽¹⁹⁾ as can be seen for 0.15 mm rev^{-1} when cutting speed changes from 40 m min^{-1} to 120 m min^{-1} . The same behavior is observed with 0.6 mm rev^{-1} . A higher density of machining voids, possibly associated with strong adhesion between work piece and tool,⁽²⁰⁾ is evidenced in both cases for the highest cutting speed condition; these results were even coincident with Ibrahim et al, who studied machinability of Ti6Al4V.⁽²¹⁾ In all cases, coalescence of surface defects were oriented in the cutting direction and showed no presence of cracking between them.

While the best surface finishing described through roughness measurements was found for the cutting condition of 0.15 mm rev^{-1} and 120 m min^{-1} as discussed in 3.1, surface integrity was the worst in terms of the amount and size of micro-defects along the machined surface.

3.4 Description of Chips and Cutting Tool Wear

Figure 10 shows some images of chips formed under different feed rates. As expected, the chips shaped with feed rates of 0.15 mm rev^{-1} , no matter the cutting speed, were the thinnest and their shape was saw-toothed. On the other hand, those chips obtained with the highest feed rates (0.3 and 0.6 mm/rev^{-1}), became segmented and discontinuous. The higher the feed rate the thicker the chip. Detailed observation of SEM and cross section images of chips allowed identifying different marks in the teeth structure. These marks were observed in all the chips and some

authors describe their formation as consequence of instabilities in the shear planes, producing yielding on high shear stress along a preferred plane. Finally, all the chips resulted magnetic which indicates that the severe deformation they suffered caused a martensitic transformation of the austenitic structure.




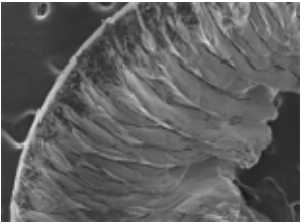
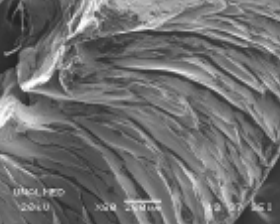
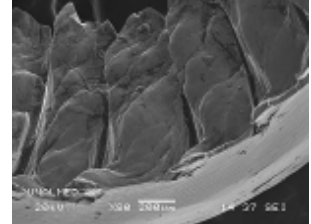
Technique	Feed rate		
	0.15 (mm rev ⁻¹)	0.3 (mm rev ⁻¹)	0.6 (mm rev ⁻¹)
OM			
SEM 80x			

Figure 10. Chip shape observation at stereomicroscope and SEM.

Figure 11a to c show SEM micrographs of the flank face of the WC/Co carbide tools for the feed rates of 0.15, 0.3 and 0.6 mm rev⁻¹ and cutting speed of 40 m min⁻¹. Figure 11 (d) to f) show stereomicroscope micrographs of the rake face for the feed rates of 0.15, 0.3 and 0.6 mm rev⁻¹ and cutting speed of 40 m min⁻¹. Evidences of chatter wear and chip breaker's wear can be observed. As the feed rate increased, the worn area also enlarged showing a severe wear condition. This behavior is attributed to the high contact temperature and the thickening and hardening of the chips.

It can be seen that the amount of adhered material in the flank face increased with the feed rate, while for lower feed rates the nitride layer was partially detached, exposing the tool substrate as shown in Figure 12c and d. This behavior indicated that for low feed rates the flank face had a faster deterioration of the cutting edge, which can be caused by a greater contact area at the chip-tool interface.

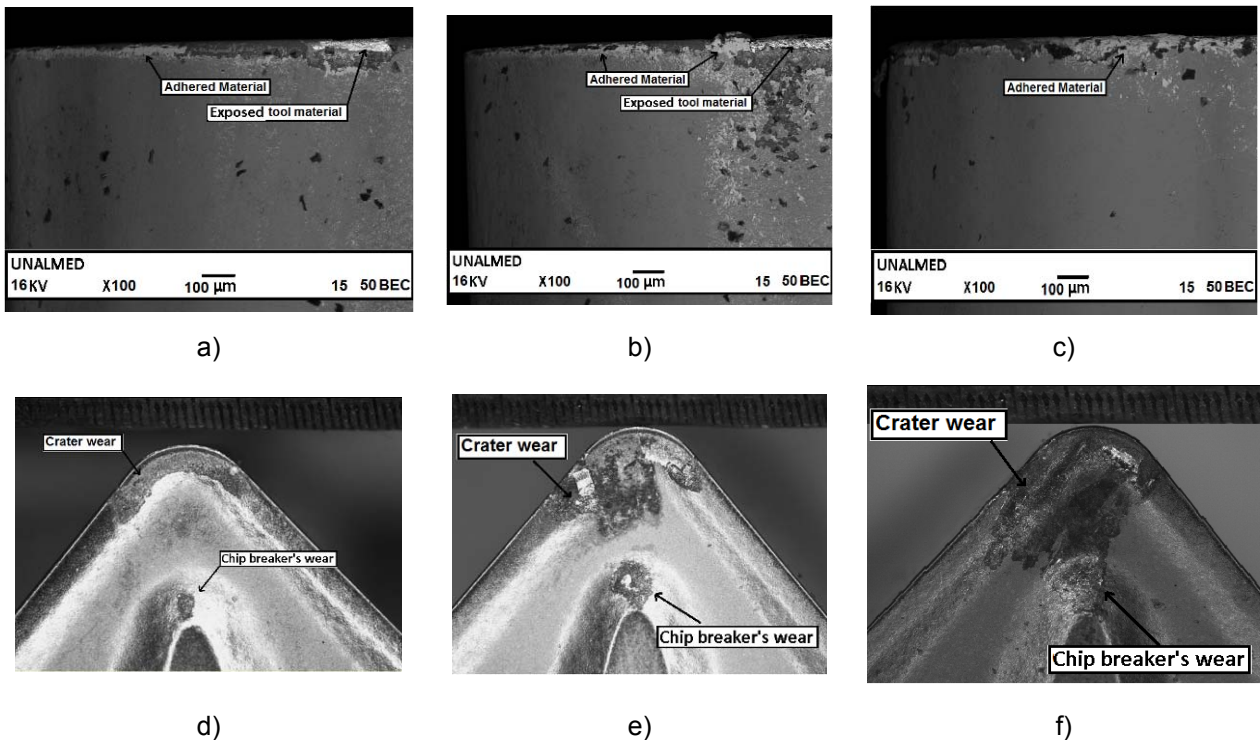


Figure 11. Flank wear and rake wear at different feed rates and cutting speed of 40 m min^{-1} . (a) 0.15 mm rev^{-1} b) 0.3 mm rev^{-1} c) 0.6 mm rev^{-1} d) 0.15 mm rev^{-1} e) 0.3 mm rev^{-1} and f) 0.6 mm rev^{-1} .

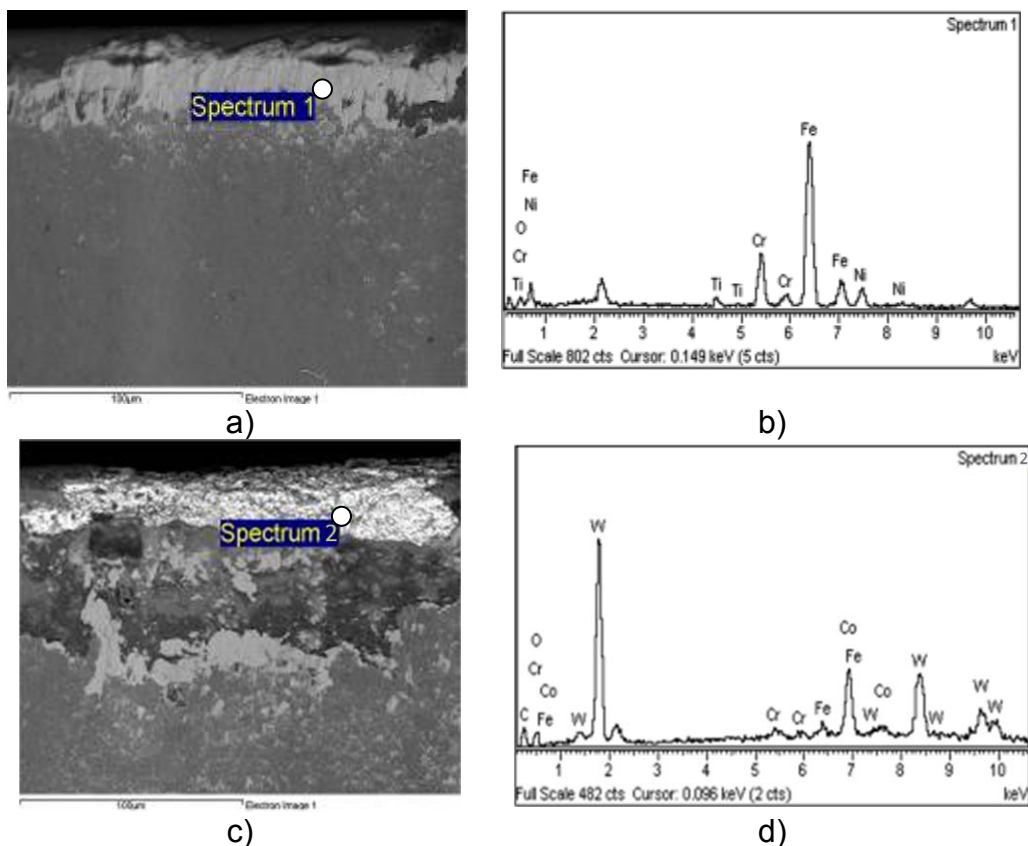


Figure 12. SEM micrograph and EDS for $V = 40 \text{ m min}^{-1}$, $f = 0.15 \text{ mm rev}^{-1}$ a) Worn flank face of the WC/Co carbide tool after machining showing AISI 304 adhered b) Chemical composition at point 1 c) Worn flank face of the WC/Co carbide tool after machining showing tool material and d) Chemical composition at point 2.

4 CONCLUSIONS

- Surface finishing of AISI 304 stainless steel after tested turning operations was mainly affected by the feed rate. The flattest surface finishing described through roughness measurements was found for the cutting condition of 0.15 mm rev⁻¹ and 120 m min⁻¹, but surface integrity was the worst in terms of the amount and size of micro-pits and marks along the machined surface. Commonly, these defects are not considered in large scale manufacturing, pointing to optimum quantity production.
- Tested machining conditions evidenced a preference in the formation of peaks rather than valleys making peak-to-valley ratio R_p/R_v and hybrid parameters ratio R_{pk}/R_{vk} better descriptors of the improvement of the surface finish, rather than R_a and R_q .
- A work hardened layer up to 60 to 70 μm beneath machined surface was measured in all tested samples. The highest microhardness values were found for a cutting condition of 0.6 mm rev⁻¹. Also, this condition showed a considerable rake face wear associated to the contact of the thickened and hardened chips during the turning operation.
- R_a and R_t were calculated according to the conventional relationships for roughness predictions of machined surfaces. It was found that R_t is the only parameter that fits with predictions but only for low feed rates.

Acknowledgments

The authors thank to Materials Characterization Laboratory at National University of Colombia, Medellín and to the Machine Tool Center at Metropolitan Technologic Institute ITM for allowing us to use their facilities.

REFERENCES

- 1 KOSA, T., 1989. Machining of Stainless Steels. Metals Handbook, ninth ed. ASM International, pp.115–133
- 2 TEKINER, Z., YESILYURT S., Investigation of the cutting parameters depending on process sound during turning of AISI 304 austenitic stainless steel.
- 3 SULLIVAN, D, COTTERELL M. Machinability of austenitic stainless steel SS303. J Mater Process Technol 2002; 124:153–9
- 4 JIANG, L., ROOS, A., LIU, P. The influence of austenite grain size and its distribution on chip deformation and tool life during machining of AISI 304L, Metall. Mater. Trans. 1997; 28A: pp. 2415–2419.
- 5 KARAMAN, I., SEHITOGLU, H., CHUMLYAKOV Y. I., MAIER, H. J. The deformation of low-stacking-fault-energy austenitic steels. JOM, 54, 7, 31-37,
- 6 IHSAN, K., MUSTAFA, K., IBRAHIM, C., ULVI, S. Determination of optimum cutting parameters during machining of AISI 304 austenitic stainless steel. Mater. Des. 25, 303–305,2004.
- 7 CEBELI, O. Turning of AISI 304 austenitic stainless steel, Journal of Engineering and Natural Sciences, 117-121, 2006
- 8 W.S. LIN , The study of high speed fine turning of austenitic stainless steel, Journal of Achievements in Materials and Manufacturing Engineering, 27, 2, 2008.
- 9 SHAW, M.C. Metal cutting principles, Oxford University Press, Ed. 1984, pp 450-542
- 10 LULA, R.A, Stainless Steel, Amerian Society for Metals, 1986, p64.
- 11 GADELMAWLA. E.S. et al, Roughness Parameters, Journal of Materials Processing Technology 123 (2002) 133-145

- 12 BOOTHROYD, D.G. Fundamentals of metal machining and machine tools, McGraw-Hill, 1975, pp. 125-142
- 13 GEORGIOS P. Petropoulos, CONSTANTINOS N. Pandazaras, J. Paulo DAVIM, Surface integrity in machining: Surface Texture Characterization and Evaluation Related to Machining, SPRINGER 2010.
- 14 DAVIM J.P. "Influencia das condicoes de corte na microgeometria das superficies obtidas por torneamento", Tese de Mestrado, Universidade do Porto, 1988-1990, pp. 110-111
- 15 B.J. GRIFFITHS, Mechanisms of white layer generation with reference to machining and deformation processes, Transactions of the ASME, Journal of Tribology 109 (1987) 525-530
- 16 CHOU, Y. K. and EVANS, C. J., "White Layers and Thermal Modeling of Hard Turned Surfaces," International Journal of Machine Tools and Manufacture, 39(12), pp. 1863-1881, 1999.
- 17 E. BRINKSMEIER, T. BROCKHOFF, Proceedings of the 2nd International German and French Conference on High Speed Machining, 1999, pp. 7–13
- 18 XICHENGWEI et al, Evolution of friction-induced microstructure of SUS 304 meta-stable austenitic stainless steel and its influence on wear behavior.
- 19 L. ZHOU, J. Shimizu, A. Muroya, H. Eda, Material removal mechanism beyond plastic wave propagation rate, Precision Engineering 27 (2003) 109–116.
- 20 GRZESIK, W., A revised model for predicting surface roughness in turning, WEAR, Vol. 194, Issues 1-2, June 1996, pages 143-148.
- 21 G. A. IBRAHIM, C.H. Che Haron and J. A. Ghani, Surface integrity of ti-6al-4v eli when machined using coated carbide tool under dry cutting condition, International Journal of Mechanical and Materials Engineering (IJMME), Vol. 4 (2009), No. 2, 191-196